Inorg. Chem. **2008**, *47*, 7424−7429

First Row Transition Metal Ion-Assisted Ammonia−Borane Hydrolysis for Hydrogen Generation

Suresh Babu Kalidindi, M. Indirani, and Balaji R. Jagirdar*

Department of Inorganic & Physical Chemistry, Indian Institute of Science, Bangalore 560 012, India

Received May 3, 2008

Ammonia−borane (AB) hydrolysis for the generation of hydrogen has been studied using first row transition metal ions, such as Co^{2+}, Ni^{2+}, and Cu^{2+}. In the cases of cobalt- and nickel-assisted AB hydrolysis, amorphous powders are formed that are highly catalytically active for hydrogen generation. Annealing of these amorphous powders followed by powder X-ray diffraction measurements revealed the presence of Co(0) and Co_2B and Ni(0) and Ni_3B, respectively. On the other hand, copper-assisted AB hydrolysis was catalyzed by in situ generated H^+ and Cu(0) nanoparticles. The reduction ability of AB for the realization of coinage metal nanoparticles from the respective metal salts has also been studied. These reduction reactions were found to be facile, affording colloids of pure metal nanoparticles. Nanoparticles prepared in this manner were characterized by UV−visible spectroscopy and high-resolution electron microscopy.

Introduction

Hydrogen has been in the limelight for the past several years from the standpoint of the so-called *hydrogen economy*. It is considered to be the best alternative to hydrocarbon fuels due primarily to its clean burning nature and environmental friendliness and also high-energy content equal to 142 MJ/kg.[1] This is three times larger than that of liquid hydrocarbons. However, storing hydrogen in large quantities for onboard applications remains a major hurdle for its widespread usage.[2] The low density of H_2 makes it difficult to store in compressed or liquefied form.

Ammonia−borane ($H_3N{\cdot}BH_3$, AB) has been attracting a great deal of attention as a hydrogen storage medium.[3] It contains 19.6 wt % of H_2, which is greater than the U.S. Department of Energy target (by 2015) of 9 wt % hydrogen for a material to be practically applicable.[4] It is a stable and safer material to handle at room temperature. The release of hydrogen from AB can be accomplished either by thermolysis or a hydrolysis route. The thermolytic generation of hydrogen from AB has been well studied. The decomposition temperatures of AB for the release of H_2 were brought down by the use of materials like nanoscaffolds,[5] ionic liquids,[6] and Ir metal complexes as catalysts.[7] The catalytic hydrolysis of AB has been studied using various transition metal catalysts.[8] Although rapid H_2 release rates have been achieved using various precious metal catalysts, there is a general desire for first row, cheap, and abundant transition metal catalysts with high stability. Recently, Xu and coworkers reported AB hydrolysis for H_2 generation catalyzed by Fe nanoparticles.[9] They found that the reduction of Fe^{2+} with $NaBH_4$ in the presence of AB resulted in amorphous Fe nanoparticles that were several times more active than crystalline Fe nanoparticles. In our search for a more abundant first-row transition-metal-based catalyst, we recently investigated the activities of nanostructured Cu, Cu_2O,

* Author to whom correspondence should be addressed. E-mail: jagirdar@ipc.iisc.ernet.in.

(1) Schlapbach, L.; Zuttel, A. *Nature* **2001**, *414*, 353.
(2) Berg, A. W. C. V.; Areán, C. O. *Chem. Commun.* **2008**, 668.
(3) Stephens, F. H.; Pons, V.; Baker, R. T. *Dalton Trans.* **2007**, 2613.
(4) Marder, T. B. *Angew. Chem., Int. Ed.* **2007**, *46*, 8116.
(5) Gutowska, A.; Li, L.; Shin, Y.; Wang, C. M.; Li, X. S.; Linehan, J. C.; Smith, R. S.; Kay, B. D.; Schmid, B.; Shaw, W.; Gutowski, M.; Autrey, T. *Angew. Chem., Int. Ed.* **2005**, *44*, 3578.
(6) Bluhm, M. E.; Bradley, M. G.; Butterick, R.; Kusari, U.; Sneddon, L. G. *J. Am. Chem. Soc.* **2006**, *128*, 7748.
(7) Denney, M. C.; Pons, V.; Hebden, T. J.; Heinekey, D. M.; Goldberg, K. I. *J. Am. Chem. Soc.* **2006**, *128*, 12048.
(8) (a) Cheng, F.; Ma, H.; Li, Chen, J. *Inorg. Chem.* **2007**, *46*, 788. (b) Ramachandran, P. V.; Gagare, P. D. *Inorg. Chem.* **2007**, *46*, 7810. (c) Clark, T. J.; Whittell, G. R.; Manners, I. *Inorg. Chem.* **2007**, *46*, 7522. (d) Chandra, M.; Xu, Q. *J. Power Sources* **2007**, *168*, 135. (e) Keaton, R. J.; Blacquiere, J. M.; Baker, R. T. *J. Am. Chem. Soc.* **2007**, *129*, 1844.
(9) Yan, J.-M.; Zhang, X.-B.; Han, S.; Shioyama, H.; Xu, Q. *Angew. Chem., Int. Ed.* **2008**, *47*, 1.

10.1021/ic800805r CCC: $40.75
Published on Web 07/23/2008

and Cu@Cu_2O nanoparticles for AB hydrolysis and found that Cu@Cu_2O or Cu_2O nanoparticles were more active than Cu^0 nanoparticles.[10]

Herein, we studied the activities of various first row transition metal ions toward AB hydrolysis for the release of H_2. The most interesting outcome of this work is that AB can reduce metal ions upon hydrolysis. In the case of Co^{2+} and Ni^{2+}, the metal powders that resulted were amorphous in nature, whereas in the case of copper, it was crystalline. The amorphous Co and Ni nanopowders were found to be catalytically active toward AB hydrolysis. We have further explored the reduction ability of AB by demonstrating the generation of coinage metal nanoparticles.

Experimental Section

Materials. Ammonia−borane was synthesized from NH_4CO_3 and $NaBH_4$ using the procedure described by Hu et al.[11] All of the metal salts $NiCl_2 \cdot 6H_2O$, $CoCl_2 \cdot 6H_2O$, $CuCl_2 \cdot 6H_2O$, $CuSO_4 \cdot 2H_2O$, $AgNO_3$, and $HAuCl_4 \cdot 3H_2O$ were obtained from S. D. Fine Chemicals Limited, India. Polyvinylpyrrolidone (PVP) was purchased from Fluka.

Instrumentation. A Perkin-Elmer Lambda 35 UV/vis spectrometer was used for recording the UV−visible spectra for the Cu, Ag, and Au colloids. Transmission electron microscope (TEM) bright field images, high-resolution TEM (HRTEM) images, and selective area electron diffraction (SAED) patterns were obtained using a TECNAI F30 transmission electron microscope. The TEM samples were prepared on carbon-coated copper grids. The samples were dried under a table lamp for more than 2 h after mounting. The powder X-ray diffraction measurements were carried out using a Philips powder X-ray diffractometer.

Ni^{2+}-, Co^{2+}-, and Cu^{2+}-Assisted AB Hydrolysis. Ammonia−borane (0.5 mmol, 16 mg) was dissolved in 20 mL of water in a Schlenk flask. A fixed mole percent of the metal ion salt ($NiCl_2 \cdot 6H_2O$, $CoCl_2 \cdot 6H_2O$, $CuCl_2 \cdot 6H_2O$) was added to this AB solution with stirring. Hydrogen evolution was monitored using a gas burette, which was connected to Schlenk flask through a water trap containing 50 mL of water. Time taken for the evolution of 1 mL of hydrogen was noted down for each milliliter. When hydrogen evolution ceased, the water levels were adjusted to equal height by moving the reservoir, and then the final reading was corrected for the water vapor pressure. The hydrolysis reaction was carried out using 7, 15, 30, 50, 75, and 100 mol % of the respective salts.

Ni, Co, and Cu Nanoparticle-Catalyzed AB Hydrolysis. The final products obtained in the Ni^{2+}-, Co^{2+}-, and Cu^{2+}-assisted AB hydrolysis reaction using 30 mol % of metal salts were isolated by filtration. The powders were washed with ethanol and dried under a vacuum. The powder XRD analysis revealed that they were made up of the respective metal and metal boride nanoparticles in the cases of Ni^{2+} and Co^{2+} but Cu and Cu_2O nanoparticles in the case of Cu^{2+}. The hydrolysis of AB (0.5 mmol) in 20 mL of water was carried out using 30 mol % of these powder samples.

Preparation of Coinage Metal Nanoparticles. $CuSO_4 \cdot 2H_2O$, $AgNO_3$, and $HAuCl_4 \cdot 3H_2O$ were used as the starting metal precursors for the preparation of Cu, Ag, and Au nanoparticles, respectively. PVP was used as a capping agent. Initially, 0.01 M stock solutions of these metal salts were prepared in 100 mL volumetric flasks. Then, a 50% AB solution was prepared in water just before the addition. In a typical experiment, the ratio of metal salt/AB/PVP was maintained at 1:5:10.

A metal salt solution (0.001 g in water) and PVP were dissolved in 30 mL of water, and then the solution was purged with argon for about 1 h. An ammonia−borane solution was added dropwise to this solution over a period of 30 min. The hydrogen evolution was observed during the addition of AB. The resultant colloids were wine red, yellow, and purple-red in color respectively in the cases of Cu, Ag, and Au nanoparticles.

Results and Discussion

Transition-metal-catalyzed $NaBH_4$ hydrolysis using metal ions and acids has been well studied by Kaufman and Sen.[12] It was found that the overall production of hydrogen using metal salts is both acid- as well as transition-metal-catalyzed. This observation is in accordance with the mechanism previously proposed by Holbrook and Twist that the reaction proceeds through the intermediacy of a metal boride complex and a metal hydride.[13] Later, Klabunde and co-workers studied the reactions of Fe^{2+},[14] Co^{2+},[15] Ni^{2+}, and Cu^{2+},[16] with $NaBH_4$ in water and diglyme. The reduction of these ions in water resulted in the formation of Fe, Co_2B, Ni_2B, and Cu nanoparticles, respectively. The reactions were quite vigorous, proceeding to completion in less than 2 min. The reduction ability of $NaBH_4$ was further explored by several other groups for the preparation of Fe,[17] Cu,[18] Ag,[19] and Au[20] nanoparticles.

With a view to realize cheap, stable, and abundant first-row transition metal catalysts for hydrogen generation from AB, we tested the activities of various metal ions. The most active ions to bring about the hydrolysis of AB were found to be Co^{2+}, Ni^{2+}, and Cu^{2+}. The hydrolysis reactions were carried out using 7, 15, 30, 50, 75, and 100 mol % of these metal ions. In most cases, aqueous AB released stoichiometric amounts of hydrogen ($H_2/H_3N \cdot BH_3 = 3.0$ mol) according to the following equation (eq 1). Reaction completion was established using ^{11}B NMR spectroscopy (see the Supporting Information).

$$H_3N \cdot BH_3 + 2H_2O \xrightarrow[298\ K]{Ni^{2+},\ Cu^{2+},\ Co^{2+}} NH_4^+ + BO_2^- + 3H_2 \quad (1)$$

Co^{2+}-Assisted Hydrolysis of AB to Generate H_2. Hydrogen evolution from an AB solution assisted by Co^{2+} showed an induction period of nearly 1 h, depending on the concentration of the starting cobalt salt used. Figure 1 shows the hydrogen evolution curves for various mole percents of

(10) Kalidindi, S. B.; Sanyal, U.; Jagirdar, B. R. *Phys. Chem. Chem. Phys.* **2008**, DOI: 10.1039/B805726E.
(11) Hu, M. G.; van Paasschen, J. M.; Geanangel, R. A. *J. Inorg. Nucl. Chem.* **1977**, *39*, 2147.
(12) Kaufman, C. M.; Sen, B. *J. Chem. Soc., Dalton Trans.* **1985**, 307.
(13) Holbrook, K. A.; Twist, P. J. *J. Chem. Soc., Dalton Trans.* **1971**, 890.
(14) Glavee, G. N.; Klabunde, K. J.; Sorensen, C. M.; Hadjapanayis, G. C. *Inorg. Chem.* **1995**, *34*, 28.
(15) Glavee, G. N.; Klabunde, K. J.; Sorensen, C. M.; Hadjapanayis, G. C. *Langmuir* **1992**, *8*, 771.
(16) Glavee, G. N.; Klabunde, K. J.; Sorensen, C. M.; Hadjapanayis, G. C. *Langmuir* **1994**, *10*, 4726.
(17) Huang, K.-C.; Ehrman, S. H. *Langmuir* **2007**, *23*, 1419.
(18) Kapoor, S.; Joshi, R.; Mukherjee, T. *Chem. Phys. Lett.* **2002**, *354*, 443.
(19) Petit, C.; Lixon, P.; Pileni, M.-P. *J. Phys. Chem.* **1993**, *97*, 12974.
(20) Brust, M.; Walker, M.; Bethell, D.; Schiffrin, D. J.; Whyman, R. *J. Chem. Soc., Chem. Commun.* **1994**, 801.

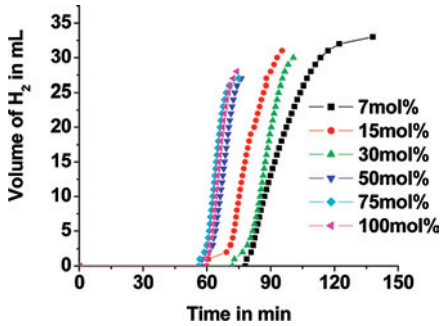

Figure 1. H_2 generation from the hydrolysis of AB (0.5 mmol) in the presence of various mole percents of $CoCl_2 \cdot 6H_2O$ in 20 mL of water.

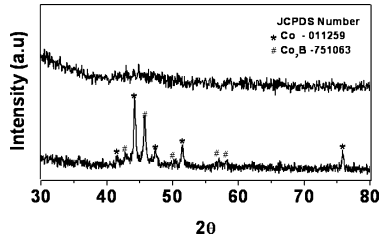

Figure 2. Powder XRD pattern of the black precipitate from the hydrolysis of AB using 30 mol % $CoCl_2 \cdot 6H_2O$ (top). Black precipitate annealed at 500 °C for 12 h under argon in a sealed capillary tube (bottom).

$CoCl_2 \cdot 6H_2O$ used. In each case, almost 3 mol of H_2 evolution was noted. In the presence of 30 and 50 mol % of the cobalt salt, H_2 evolution was complete in ca. 30 min, whereas it took a much longer time, 45 and 36 min, when the starting concentration of the Co^{2+} was 7 and 15 mol %, respectively. When the hydrogen evolution ceased, black precipitates settled at the bottom of the flask. This powder was isolated under Ar in the case of the reaction with 30 mol % of Co^{2+} via filtration and was washed several times with ethanol and dried under a vacuum. The powder X-ray diffractogram of this sample was devoid of any sharp peaks, indicating its amorphous nature. Therefore, the powder was annealed at 500 °C for 12 h under argon in a sealed capillary tube. The powder pattern of the annealed sample exhibited peaks corresponding to Co and Co_2B (Figure 2). For the reactions with 7, 15, and 30 mol % of cobalt salt, the supernatant solutions were colorless. The evaporation of water from the supernatant solution by heating it at ca. 100 °C for a few hours gave a white crystalline solid that was found to be $B(OH)_3$ by FTIR spectroscopy. A concentration of 30 mol % of the cobalt salt was found to be optimum for the generation of 3 mol of H_2 in 30 min.

Ni^{2+}-Assisted Hydrolysis of AB to Generate H_2. As in the case of cobalt, Ni^{2+}-assisted AB hydrolysis showed an induction period of ca. 3 h. Before the onset of H_2 evolution, a black material was deposited on the reaction vessel. Figure 3 shows the H_2 evolution curves by AB hydrolysis using various mole percents of $NiCl_2 \cdot 6H_2O$. The final black precipitate that resulted was isolated in the case of the reaction with 30 mol % of the nickel salt. The XRD pattern of this powder exhibited very broad and weak peaks, indicating its amorphous nature. Upon annealing the sample at 500 °C for 12 h, the powder XRD pattern revealed sharp peaks corresponding to both Ni and Ni_3B (Figure 4). A thin film of Ni was deposited on the walls of the reaction flask

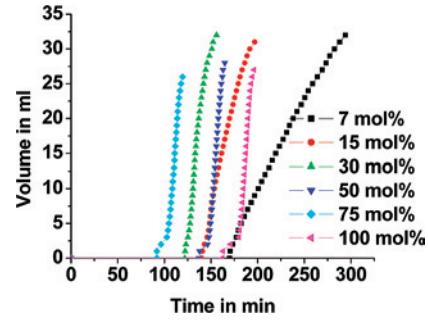

Figure 3. H_2 generation from the hydrolysis of AB (0.5 mmol) in the presence of various mole percents of $NiCl_2 \cdot 6H_2O$ in 20 mL of water.

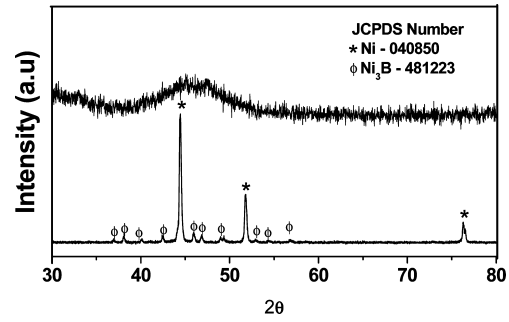

Figure 4. Powder XRD pattern of the precipitate from the hydrolysis of AB using 30 mol % $NiCl_2 \cdot 6H_2O$ (top). Precipitate annealed at 500 °C for 12 h under argon in a sealed capillary tube (bottom).

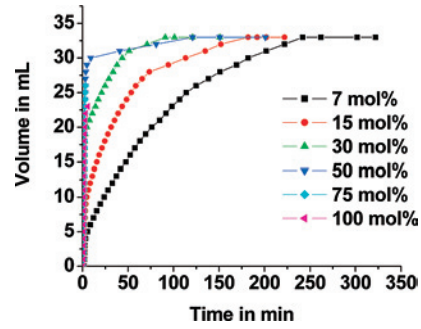

Figure 5. H_2 generation from the hydrolysis of AB (0.5 mmol) in the presence of various mole percents of $CuCl_2 \cdot 6H_2O$ in 20 mL of water.

in the case of reactions with higher mole percents (<50 mol %) of the nickel salt. In addition, the supernatant solutions in these cases were pale green in color. Upon removal of the water by evaporation, the solid residue that was obtained contained both anhydrous $NiCl_2$ and boric acid. This suggests that some of the nickel salt remained unreacted in these cases. On the other hand, reactions with 7, 15, and 30 mol % of Ni^{2+} gave supernatant solutions that were colorless. A workup of these solutions gave colorless solid products of $B(OH)_3$, as evidenced by FTIR spectroscopy. A total of 30 mol % of Ni^{2+} was found to be optimum, in which case, 3 mol of H_2 were liberated in less than 35 min.

Cu^{2+}-Assisted Hydrolysis of AB to Generate H_2. Unlike Co^{2+} and Ni^{2+}, hydrogen evolution took place almost instantaneously upon the addition of $CuCl_2 \cdot 6H_2O$ to an aqueous solution of AB. Figure 5 shows the hydrogen evolution curves for Cu^{2+}-assisted AB hydrolysis. The addition of 7, 15, 30, and 50 mol % of Cu^{2+} to an AB solution resulted in a color change from blue to brown and then to dark brown and finally to black, accompanied by

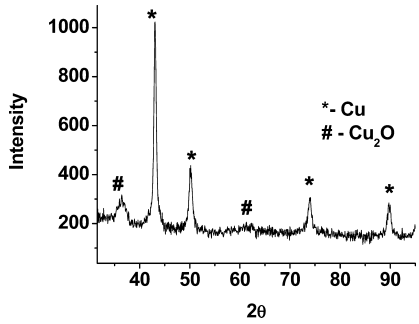

Figure 6. Powder XRD pattern of the precipitate from the hydrolysis of AB using 30 mol % $CuCl_2 \cdot 6H_2O$.

Table 1. Activities of Co^{2+}, Ni^{2+}, and Cu^{2+} Ions Towards Hydrogen Generation via AB Hydrolysis[a]

metal salt mol %	$CoCl_2 \cdot 6H_2O$		$NiCl_2 \cdot 6H_2O$		$CuCl_2 \cdot 6H_2O$	
	$T_{I.P.}$	T_{H2}	$T_{I.P.}$	T_{H2}	$T_{I.P.}$	T_{H2}
7	78	45	170	125	2	168
15	60	36	140	57	2	112
30	72	29	112	34	∼1	51
50	57	20	137	28	∼1	9
75	56	19	92	28	<1	11
100	59	16	162	35	<1	6

[a] $T_{I.P.}$: induction period in min. T_{H2}: time taken for H_2 evolution in min.

the evolution of 3 mol of H_2. However, the use of 75 and 100 mol % of the copper salt afforded a dark brown precipitate, accompanied by a less than stoichiometric amount of H_2, as per eq 1. The precipitate obtained in the reaction with 30 mol % of the copper salt was isolated. Unlike the cases of Co^{2+} and Ni^{2+}, this powder sample was found to be crystalline. The XRD pattern revealed the presence of Cu and Cu_2O (Figure 6). We noted that, at higher concentrations of AB, Cu^{2+} was completely reduced to Cu(0). The presence of Cu_2O is due to the surface oxidation of Cu(0), which could not be avoided.

Comparison of the Activities of Co^{2+}, Ni^{2+}, and Cu^{2+} Toward AB Hydrolysis. The activities of Co^{2+}, Ni^{2+}, and Cu^{2+} ion-assisted hydrolysis of AB are summarized in Table 1. In the cases of Co^{2+}- and Ni^{2+}-assisted AB hydrolysis, no clear trends in the induction period for the generation of the catalytically active species were apparent. The induction periods were roughly 1 h and 2−3 h respectively for Co^{2+} and Ni^{2+}, no matter what the starting concentrations of the respective metal salts used were. For all three cases, the time taken for H_2 liberation followed a regular trend: an increase in the mole percent of the starting metal salt (up to 50 mol %) led to faster H_2 release. However, for concentrations >50 mol % of the metal salt, no trend was apparent in all three cases, which is unclear at this time. Without taking into account the induction period, it is apparent that Co^{2+} is more active than Ni^{2+} and Cu^{2+} in the case of reactions using 7, 15, and 30 mol % of the respective salt. However, at higher mole percents of the ions, we found that Cu^{2+} is more active than Co^{2+} and Ni^{2+}. In the case of Cu^{2+}, ammonia−borane hydrolysis was found to be fast initially, slowing down after ca. 5 min. We also monitored the pH changes during the hydrolysis reactions. While the pH remained within the 8.5−9.0 range in the case of Co^{2+} and Ni^{2+} systems, large variations in the pH were noted in the case of the Cu^{2+}

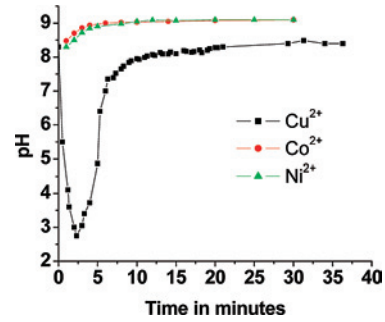

Figure 7. Changes in pH during Co^{2+}-, Ni^{2+}-, and Cu^{2+}-assisted (15 mol % in each case) AB hydrolysis.

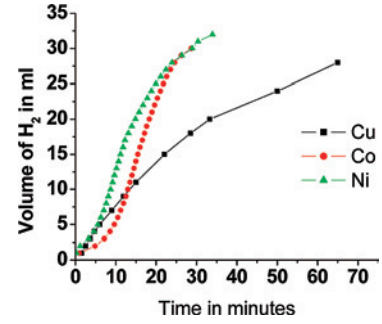

Figure 8. Hydrogen generation by the hydrolysis of AB (0.5 mmol) using amorphous Co and Co_2B; Ni and Ni_3B and polycrystalline Cu nanoparticles (metal/AB = 0.3).

system. Figure 7 shows the pH changes for the 15 mol % Cu^{2+}-assisted AB hydrolysis. It is apparent that large quantities of H^+ production take place soon after the addition of Cu^{2+} during the initial 2−3 min, which is responsible for the initial rapid H_2 evolution. Acid-catalyzed AB hydrolysis reaction kinetics have been found to be quite fast.[21] After about 5 min of reaction time, the hydrogen evolution slowed down, and the reaction was catalyzed by in situ generated Cu nanoparticles. We recently reported that Cu@Cu_2O and Cu_2O nanoparticles are active catalysts for the generation of hydrogen from AB; however, Cu nanoparticles are not as active.[10] The recyclability of the copper catalyst obtained in the present work was tested and found to be quite good; we found no decrease in the activity for up to eight cycles.

Unlike the case of Cu^{2+}, the pH remained in the range 8.5−9.0 (Figure 7) during the course of the reaction when cobalt and nickel salts were employed. This suggests that the mechanism is quite different for the Co^{2+}- and Ni^{2+}-assisted AB hydrolysis in comparison to that of Cu^{2+}. The visual observation of H_2 evolution that is initiated only after the formation of amorphous black material in the cases of Co^{2+}- and Ni^{2+}-assisted AB hydrolysis suggests that they are the catalytically active species. In order to establish this further, we isolated the black amorphous materials in both cases and tested their activities for AB hydrolysis. Figure 8 shows the hydrogen evolution curves using the black amorphous materials for AB hydrolysis. In both of these cases, the activities are more or less the same, and so were the recyclabilities. The activities of the catalysts remained unchanged for up to eight cycles. The powder XRD pattern of the black amorphous materials upon annealing evidenced

(21) Kelly, H. C.; Marriott, V. B. *Inorg. Chem.* **1979**, *18*, 2875.

the presence of Co and Co_2B and Ni and Ni_3B, respectively.

Thus, these are examples of first-row transition metal catalysts that produce 3 mol of H_2 within 30 min via the hydrolysis of AB. On the other hand, copper nanoparticles (protected from air) that were isolated from the Cu^{2+}-assisted AB hydrolysis reaction were found to effect slower H_2 evolution compared to Cu^{2+}, which is in accordance with our postulate of initial acid catalysis.

Coinage Metal Nanoparticles Using Ammonia−Borane. The observation that Cu^{2+} ions got reduced to Cu^0 upon the hydrolysis of AB prompted us to explore further the reducing ability of AB. Thus, we prepared Cu, Ag, and Au nanoparticles from $CuSO_4 \cdot 2H_2O$, $AgNO_3$, and $HAuCl_4 \cdot 3H_2O$, respectively, using AB as the reducing agent. A well-known, conventional reducing agent usually employed for nanoparticles synthesis, $NaBH_4$ suffers from certain drawbacks such as its instability in water, faster reaction rates which can lead to uncontrollable particle sizes, and the formation of water-soluble impurities like NaCl that are very difficult to remove, especially when water is employed as the reaction medium. Some of these difficulties can be overcome by using AB as the reducing agent in place of $NaBH_4$. Ammonia−borane is stable toward hydrolysis in aqueous solutions for at least 4 days. No water-soluble impurity like the one obtained in $NaBH_4$ reduction is obtained. Recently, Manners and co-workers reported the formation of 2 nm Rh nanoparticles when [Rh(μ-Cl)(1,5-cod)]$_2$ was treated with $Me_2NH \cdot BH_3$.[22]

The copper colloids obtained via reduction of Cu^{2+} to Cu^0 using AB were wine red in color, exhibiting a surface plasmon resonance (SPR) at 560 nm (Figure 9a). For copper nanoparticles of 10 nm diameter, the UV−visible spectrum is characterized by a broad SPR at 570 nm.[23] Subtle variations in the position of the SPR are due to the different surfactants present (here, PVP) at the surface of the particles and the dielectric properties of the solvent.[24] The colloids were found to be quite stable toward oxidation for at least 2 days, in the presence of excess AB. This is due to the presence of a constant H_2 atmosphere generated via very slow hydrolysis of AB catalyzed by pure Cu^0 nanoparticles. The colloids were also stable toward precipitation of Cu nanoparticles for months. The TEM bright field image (Figure 9b) revealed the presence of 3−7 nm particles with an average particle size of 4.3 nm (Figure 9c). The HRTEM image (Figure 9d) showed lattice fringes corresponding to the (111) plane of the face-centered-cubic (FCC) copper phase. The SAED pattern (Figure 9e) shows a ring pattern: all four rings match with the lattice planes (111), (200), (220), and (311) of the FCC copper phase. From these findings, we conclude that these samples are comprised of pure crystalline Cu^0nanoparticles.

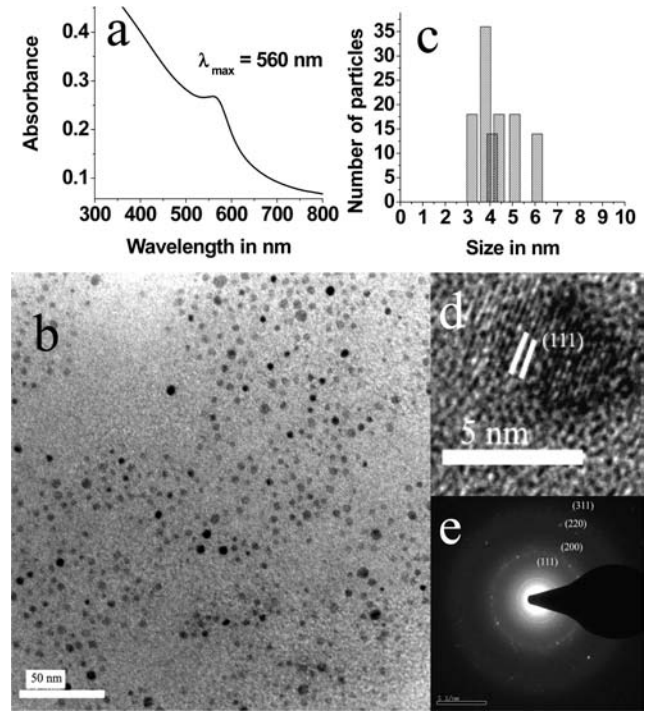

Figure 9. (a) UV−visible spectrum of Cu colloid. (b) TEM bright field image of Cu colloid. (c) Histogram showing the particle size distribution. (d) HRTEM image of Cu(0) nanoparticle. (e) SAED pattern of Cu(0) nanoparticles.

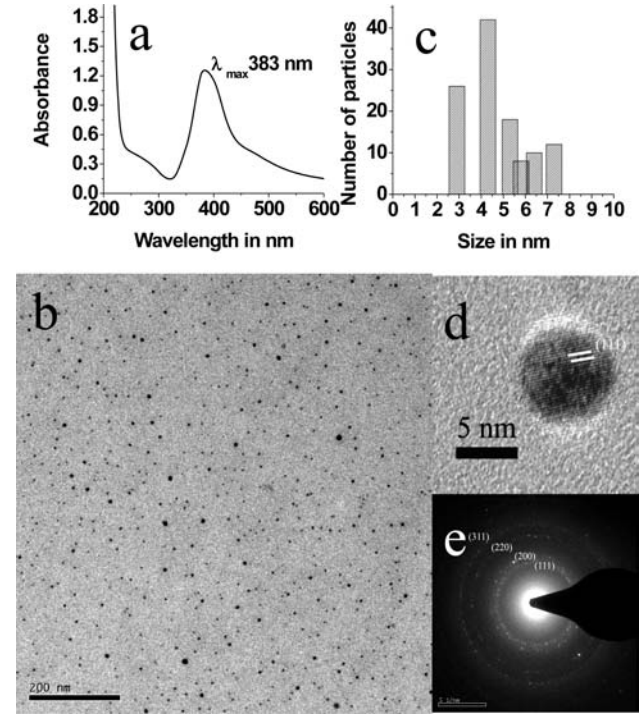

Figure 10. (a) UV−visible spectrum of Ag colloid. (b) TEM bright field image of Ag colloid. (c) Histogram showing the particle size distribution. (d) HRTEM image of Ag(0) nanoparticle. (e) SAED pattern of Ag(0) nanoparticles.

(22) (a) Jaska, C. A.; Temple, K.; Lough, A. J.; Manners, I. *J. Am. Chem. Soc.* **2003**, *125*, 9424. (b) Jaska, C. A.; Manners, I. *J. Am. Chem. Soc.* **2004**, *126*, 9776. (c) Fulton, J. L.; Linehan, J. C.; Autrey, T.; Balasubramanian, M.; Chen, Y.; Szymczak, N. K. *J. Am. Chem. Soc.* **2007**, *129*, 11936.

(23) Creighton, J. A.; Eadon, D. G. *J. Chem. Soc., Faraday Trans.* **1991**, *87*, 3881.

(24) (a) Huang, H. H.; Yan, F. Q.; Kek, Y. M.; Chew, C. H.; Xu, G. Q.; Ji, W.; Oh, P. S.; Tang, S. H. *Langmuir* **1997**, *13*, 172. (b) Ziegler, K.; Doty, R. C.; Johnston, K. P.; Korgel, B. A. *J. Am. Chem. Soc.* **2001**, *123*, 7797. (c) Rothe, J.; Hormes, J.; Bönnemann, H.; Brijoux, W.; Siepen, K. *J. Am. Chem. Soc.* **1998**, *120*, 6019.

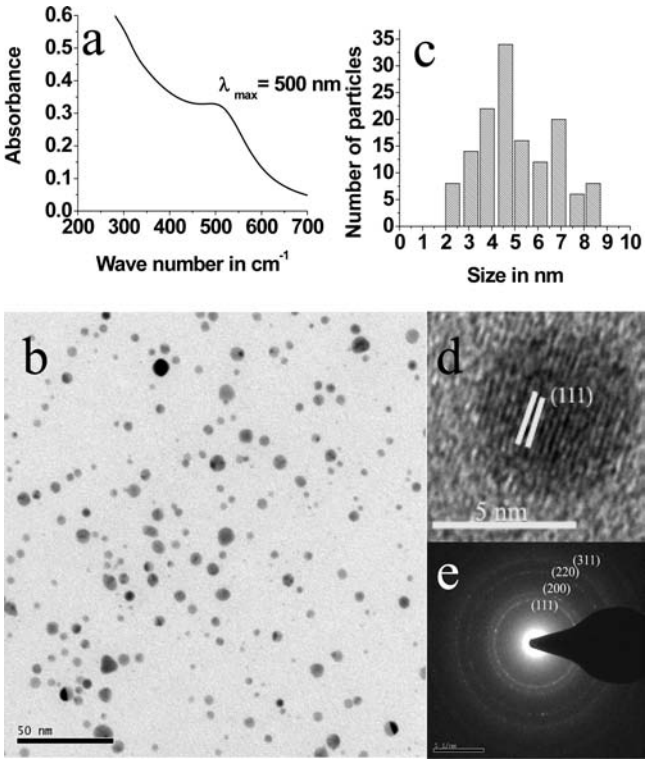

Figure 11. (a) UV−visible spectrum of Au colloid. (b) TEM bright field image of Au colloid. (c) Histogram showing the particle size distribution. (d) HRTEM image of Au(0) nanoparticle. (e) SAED pattern of Au(0) nanoparticles.

We also prepared yellow-colored silver colloids by the reduction of $AgNO_3$ using AB in the presence of PVP as the surfactant. These samples exhibited an SPR at 383 nm (Figure 10a). Silver nanoparticles of 10 nm diameter exhibit the SPR at 390 nm.[23] The blue shift of the SPR in our samples could be attributed to the smaller particle size. These colloids were found to be stable for months. The TEM bright field (BF) image (Figure 10b) showed the presence of spherical particles with an average diameter of 4.7 nm (Figure 10c). The HRTEM image (Figure 10d) and the SAED pattern (Figure 10e) further support the presence of pure crystalline FCC Ag^0 nanoparticles.

In a manner analogous to the reduction of the copper and silver salts for the realization of the respective metal nanoparticles, we were successful in obtaining Au nanoparticles via reduction of $HAuCl_4 \cdot 3H_2O$. The resultant purple-red gold colloids showed a broad SPR at 500 nm (Figure 11a.) The Au colloids were also found to be quite stable toward precipitation for several months, similar to the Cu and Ag systems. Unlike Cu and Ag, the Au nanoparticles obtained by this method were found to be polydisperse, as evidenced by the TEM BF image (Figure 11b) with particle sizes ranging from 2 to 9 nm. The average particle size in this case is 5.1 nm (Figure 11c). The HRTEM image (Figure 11d) and the SAED pattern (Figure 11e) further support the presence of pure crystalline Au^0 nanoparticles.

Conclusions

Several first row transition metal ions assist the hydrolysis of AB under very mild conditions for the generation of H_2. Co^{2+} and Ni^{2+} assisted AB hydrolysis show some induction period during which time catalytically active amorphous species are formed that show exceptional activities. The Cu^{2+}-assisted hydrolysis of AB was catalyzed by both in situ generated H^+ and Cu(0) nanoparticles. Of the three cases, the cobalt system was found to be more active than the nickel and the copper systems, without taking into consideration the induction period. The ammonia−borane reduction of coinage metal salts resulted in the respective metal nanoparticles under very mild conditions. Our work is, therefore, a demonstration of the deployment of cheap and abundant and, at the same time, stable first row transition metal catalysts for the generation of H_2 from AB via hydrolysis.

Acknowledgment. We are grateful to the Council of Scientific and Industrial Research, India, for financial support. We thank the I.I.Sc. Institute Nanoscience Initiative and the Solid State and Structural Chemistry Unit, I.I.Sc., for allowing us to access the microscopic facilities and the powder X-ray diffractometer, respectively. S.B.K. thanks the CSIR for a fellowship.

Supporting Information Available: ^{11}B NMR spectrum showing the formation of $B(OH)_3$ and ^1H NMR spectra showing the production of H_2 and the formation of NH_4^+ in the transition metal ion-assisted hydrolysis of AB. This material is available free of charge via the Internet at http://pubs.acs.org.

IC800805R